On the Paranal Surface Layer

Jorge Melnick, Marc Sarazin, Julio Navarrete, & Gianluca Lombardi

1 Prolegomenon

The image quality delivered by the VLT Unit Telescopes (UT's) is always better, and often much better, than the seeing measured by the Paranal DIMM. This rather *inconvenient discrepancy* is thought to be due to the presence of a thin ($\Delta h < 20m$) layer of turbulent air that is seen by the DIMM but not by the UT's (Sarazin et al. 2008). The presence of this *Surface Layer* on Paranal has led some pundits to question the long term stability of the exceptional atmospheric conditions of Paranal, which would suggest that other sites in the area may not be valid alternatives for the E-ELT. The fact of the matter, however, is that while the seeing measured by the DIMM has degraded over the past 10 years, the image quality delivered by the UT's has at worst remained constant, and at best improved over the same period of time. So the real question we need to answer is what determines the height of the surface layer, and how sensitive is this mechanism to the effects of climate change. In this report we address these fundamental questions.

2 The Rise and Fall of hot air

The Schwarzschild (1958) criterion can be used to investigate the vertical stability of the atmosphere near the ground level. Suppose we have a bubble of air that has a slightly higher temperature than the surrounding medium. At the ground level the ambient pressure and density are (P_0, ρ_0) and the conditions inside the bubble are the primed quantities. At an altitude h above the ground, the ambient conditions are (P_1, ρ_1) and again the conditions in the bubble are primed.

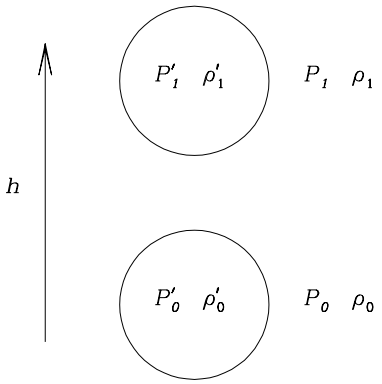

Figure 1: *A bubble of hot air raises from the ground to a new position at an altitude h. As it raises it expands adiabatically such that at the new position it is in pressure equilibrium with the ambient air.*

Assuming that we allow the bubble to expand adiabatically such that in the new position (h) it is in pressure equilibrium with the ambient air, the following equalities apply:

$$\begin{aligned} P'_0 &= P_0 \\ \rho'_0 &= \rho_0 \end{aligned} \tag{1}$$

$$P_1' = P_1$$

In order to determine the new value for the density inside the bubble, we need to use the ideal gas equation, $PV = NkT$, and the condition that the expansion is adiabatic,

$$\Delta Q = \Delta W + \Delta E = 0$$

or equivalently,

$$\frac{dW}{dV} = -\frac{dE}{dV}$$

where ΔW is the work done by the expansion of the bubble. The internal energy of the bubble is $E = qNkT$ where q is the polytropic index of the gas (5/2 for air). Remembering that $dW = PdV$ we then get that,

$$qNk\frac{dT}{dV} = -P$$

and using the ideal gas equation,

$$\frac{dT}{T} = \frac{dP}{P} + \frac{dV}{V} \tag{2}$$

we finally derive the expression for the adiabatic change in the pressure:

$$V\frac{dP}{dV} + \gamma P = 0$$

or for the density,

$$\frac{1}{\gamma}\frac{dP}{P} = \frac{d\rho}{\rho} \tag{3}$$

where $\gamma = \frac{q+1}{q}$ is the ratio of specific heats $\frac{c_P}{c_V}$. Thus, the density of the bubble at the new position is

$$\rho_1' = \rho_1(\frac{P_1}{P_0})^{\frac{1}{\gamma}} \tag{4}$$

The Schwazschild criterion tells us that the bubble will continue to raise if $\rho_1' < \rho_1$. Using eq. (1) to eliminate the primes, the stability condition becomes $\rho_1 < \rho_o(\frac{P_1}{P_0})^{1/\gamma}$. Turning this inequality into differential form ($\rho_1 = \rho_0 + d\rho; P_1 = P_0 + dP$) and expanding to first order in $\frac{d\rho}{\rho}$ and $\frac{dP}{P}$ we get,

$$\frac{1}{\gamma}\frac{1}{P}\frac{dP}{dh} < \frac{1}{\rho}\frac{d\rho}{dh}$$

which using the perfect gas equation (2) becomes the famous Schwarzschild criterion,

$$-(1 - \frac{1}{\gamma})\frac{T}{P}\frac{dP}{dh} > -\frac{dT}{dh} \tag{5}$$

The left hand of the equation is called the adiabatic temperature gradient in stellar physics, while the right hand term is the actual temperature gradient: the layer is stable if the actual temperature gradient is *lower*

than the adiabatic gradient in absolute terms. One needs to be very careful with the signs here. For stellar interiors both the pressure and the temperature gradients are negative, so this formula is usually written with minus signs such that both sides of the inequality are strictly positive. The earth atmosphere, on the other hand, has layers where the temperature gradient is inverted, so the right-hand term of the inequality can be positive or negative.

Meteorologists prefer to introduce the potential temperature, which eliminates the pressure dependence on the temperature,

$$\theta = T(\frac{1000}{P})^{\frac{\gamma-1}{\gamma}} \tag{6a}$$

with the pressure in millibars, so the Schwarzschild criterion tells us that atmospheric layers are stable if

$$d\theta/dh > 0 \tag{6b}$$

For air $\gamma = 7/5$ so $(\gamma - 1)/\gamma = 2/7 = 0.286$.

3 Going with the Flow

3.1 The Reynolds number

In a laminar flow the fluid is stratified in *laminae*. The velocity gradient across these laminae, dU/dh, is a well behaved function which is low in the boundaries and highest in the center of the flow. (Some authors define fluids as materials that flow in that way.) If the speeds are very large, the flow develops turbulence. Viscous drag shears (deforms) the flow perpendicular to the speed gradient and acts against the curling velocity shear. Turbulence sets-in when the inertial forces are much larger than the shear forces due to viscosity. The ratio of these two forces is the Reynolds number,

$$\Re = \frac{\rho U^2 L^2}{\mu U L} = \frac{UL}{\nu} \tag{7}$$

where U is the flow speed, ρ_0 is the density, and μ is the friction coefficient. $\nu = \mu/\rho$ is the *kinematic viscosity* and L is the characteristic dimension of the flow, which is generally determined by its boundaries. For air at 15^oC $\nu \sim 1.5 \times 10^{-5} m^2/s$ while for water $\nu \sim 10^{-6} m^2/s$. Experimentally it is verified that flows become turbulent when $\Re > 2000$. At slow speeds (a few meters per second) winds become turbulent when perturbed even by very small obstacles, while at very high speeds winds are unstable and may develop turbulence spontaneously (Tatarski, 1961).

3.2 The Richardson number

In typical conditions in the Earth's atmosphere viscous forces are negligible compared to buoyancy forces generated by gravity and heat. Therefore turbulence sets-in when the inertial forces are larger than the buoyancy. The Richardson number $\mathcal{R}_i$ is defined as the ratio between these forces. In the simplest approximation the buoyancy is given by the Archimedes force $g\rho V$ and the inertial force is $\rho U^2 A$, where A is the characteristic area and V the corresponding volume,

$$\mathcal{R}_i = \frac{\text{buoyancy force}}{\text{inertial force}} = \frac{gh}{U^2}$$

h is the altitude above ground. A finer analysis must consider the fact that in a stratified medium such as the atmosphere there is not only a pressure gradient induced by gravity, but heat is transported vertically, and the density, temperature, humidity and velocity vary with h. Thus,

$$\mathcal{R}_i = -\frac{g}{\rho}\frac{\frac{d\rho}{dh}}{(\frac{dU}{dh})^2} \tag{8}$$

Since it is much easier to measure temperature than density, meteorologists prefer to use the *potential temperature* θ defined above instead of the density. For an ideal gas $d\rho/\rho = -d\theta/\theta$, so the Richardson number is usually calculated as, [1]

$$\mathcal{R}_i = \frac{g}{\theta}\frac{\frac{d\theta}{dh}}{(\frac{dU}{dh})^2} \tag{9}$$

The magical Richardson number below which inertial stresses dominate over buoyancy forces is 0.25. Thus, the flow is unstable to turbulence when $\mathcal{R}_i < 0.25$. Notice however that there is hysteresis, so the criterion to regain stability after turbulence is $\mathcal{R}_i > 1$ (e.g. Stull, 1988).

3.3 The Kolmogorov cascade

Turbulence is generally characterized by the structure function (a sort of two-point correlation function), which for a homogeneous isotropic flow is

$$D_U(\Delta r) =< [U(r) - U(r+\Delta r)]^2 >$$

the velocity difference between two elements separated by a distance Δr (or a time lag Δt) squared averaged over all points separated by Δr. This definition applies not only for the velocities, but also to other flow variables such as the temperature, the concentration of aerosols, or the index of refraction. The relevant variable is usually denoted as a subscript, in this case U. For discretely sampled quantities, the structure function is computed as:

$$D_U(a) = \frac{1}{N-j}\sum_{i=1}^{N-j}(U_i - U_{i+j})^2$$

where $a = j\Delta t$ or $j\Delta r$. In a turbulent cascade, energy is injected at some scale L (for example by wind), and dissipated at a scale l where viscous forces dominate over inertial forces. Kolmogorov assumed that in the *inertial* range $l < a < L$, energy is conserved and that the rate of kinetic energy transfer ($\epsilon = dU^2/dt$) is independent of eddy size. Thus, $D_U(a)$ would have the functional form $D_U(a) = C\epsilon^\alpha a^\beta$ where C is a dimensionless constant, and the exponents α and β must be determined such that D_U has the correct dimensions (velocity squared). Following this dimensional analysis, Kolmogorov deduced his famous law,

$$D_U(a) = C\epsilon^{2/3}a^{2/3}$$

The power spectrum of the turbulence is the Fourier transform of the structure function,

$$\mathcal{P}_U(k) = \int_{-\infty}^{+\infty} D_U(a)e^{-iak}da = B\epsilon^{2/3}k^{-5/3}$$

where as usual $k = 2\pi/\lambda$ is the spatial frequency. B is a dimensionless constant. The quantity $B\epsilon^{2/3}$ is usually denoted C_U^2 (actually C_{U^2} in the meteorology literature) and depends on the altitude of the turbulent layer. Thus, the power spectrum of the velocity structure function is,

[1] Strictly, the virtual potential temperature, $\theta_v = \theta(1 + 0.00061r)$, where r is the mixing ratio of dry air and water vapor, should be used to calculate the Richardson number because water vapor is more buoyant than dry air. However, for the typical relative humidity of Paranal ($q < 20\%$), $r = q * r_{sat} \lesssim 2$g/kg, while the relative humidity changes by at most a few percent from 2m to 30m, so $\theta_v = \theta$ is a very good approximation for typical conditions on Paranal.

$$\mathcal{P}_U(h,k) = C_U^2(h) k^{-5/3}$$

Kinetic energy is injected into the flow at a spatial frequency $k_L = 2\pi/L$ at a rate ϵ, and dissipated at a scale $k_l = 2\pi/l$ at the same rate. The (constant) kinetic energy transfer rate is $\epsilon \sim U^2/\Delta t$ and the characteristic time is $\Delta t \sim U/a$, so $\epsilon \sim U^3/a$. By definition at the dissipation scale (l) $\Re = 1$, so $\nu = U_l^2 l$ and $l = (\nu^3/\epsilon)^{1/4}$. Thus, the following scaling relations follow from the definition of the Reynolds number (e.g. Tatarski, 1961)

$$\begin{aligned} \frac{L}{l} &= \Re^{3/4} \\ \frac{\Delta t_L}{\Delta t_l} &= \Re^{1/2} \\ \frac{U_L}{U_l} &= \Re^{1/4} \end{aligned} \tag{10}$$

For a typical wind speed of $U \sim 5$m/s, (external) scale $L \sim 100$m, and air at 15°C, $\Re \sim 10^8$ so $l \sim 0.25$mm and $\Delta t_l \sim$4ms. At the dissipation scale the eddies are moving at a few cm/s.

3.4 Optical turbulence

In ground-based astronomy we observe the distortions of a plane wave that propagates through the turbulent atmosphere. In order to calculate these distortions we need to know the power spectrum of the index of refraction n, which is related to $\mathcal{P}_U(h,k)$, but is not the same since n also depends on pressure, temperature, and humidity. Balloon measurements show that the fluctuations in n are layered in relatively thin turbulent sheets at different altitudes "sandwiched" by much thicker regions of stable conditions. As discussed above, the turbulent layers are characterized by having small Richardson numbers $\mathcal{R}_i < 0.25$. Optical turbulence arises in these unstable layers because vorticity mixes parcels of air of different temperatures creating fluctuations in the index of refraction. Balloon experiments show that the external scale (L_U) of the velocity field in these layers is of the order of a few hundred meters $L_U \sim 500$m, but experimental evidence both remote and in-situ with balloons indicate that the sheets showing *optical turbulence* (i.e. fluctuations of n) appear to be considerably thinner (e.g. a few meters, $L_0 \sim 5$m; Coulman, Vernin, & Fuchs, 1995, and references therein). However, there is disagreement among the experts about such low values for the external or *outer* scale of optical turbulence.

An independent way of estimating L_0 is to use the Von Karman model (e.g. Tokovinin, 2002). As stressed by Tokovinin, fits to the von Karman model give the wavefront outer scale Ł$_0$ that describes the wavefront statistics after propagation through the *whole* atmosphere. Thus, with the caveats that the Von Karman model has not been verified, and that the wavefront outer scale should be proportional to the geophysical outer scale, but not the same, the experimental evidence indicates that L_0 ranges from $\sim$ 10m to $\sim$ 100m with typical values of $\sim$ 20m.

4 Paranal

4.1 Schwarzschild criterion

Figure 2 shows the statistics of the actual temperature gradient for the first 30m over Paranal.

The mean temperature gradient over Paranal between ground (2m) and 30m altitude at night is

$$\frac{dT}{dh} = +0.0168 \pm 0.0146(\sigma)\,\mathrm{deg}/m$$

and the median temperature difference is $\Delta T = +0.4$ degrees. For comparison, the adiabatic temperature gradient is

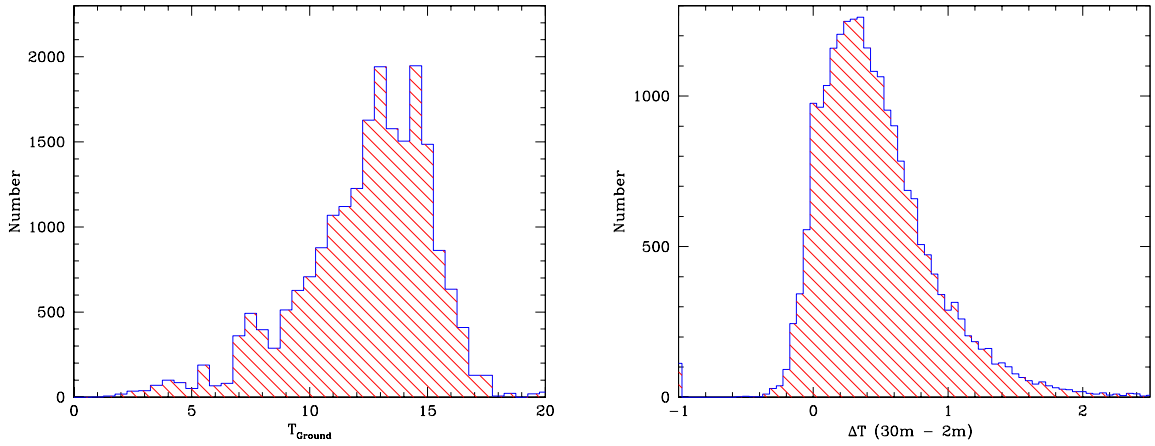

Figure 2: (left) *Distribution of temperature at 2m on Paranal.* (right) *Difference in temperature between the ground and 30m altitude.*

$$\frac{dT}{dh} = -\frac{(\gamma - 1)}{\gamma}\frac{g m_A}{k} = -0.0098 \text{ deg/m}$$

where m_A is the mean molecular weight of air ($\sim$ 29amu) and g is the gravitational acceleration. Thus, 30m above ground one would expect the air to be about 0.3 degrees cooler, whereas we observe it to be about 0.4 degrees warmer. The mean potential temperature gradient in the first 30m above Paranal is

$$\frac{d\theta}{dh} = 0.017 \text{ deg/m} \tag{10}$$

so the atmosphere should be stable against convective turbulence over the first 30m during night time. Paranal weather is seen to be remarkably stable between day and night (and in fact from season to season).

4.2 Richardson number

In order to compute the Richardson number $\mathcal{R}_i$ we need to know the wind shear dU/dh and the gradient in potential temperature $d\theta/dh$. As mentioned above for the moment we only have thermometers at 2m and 30m so a fortiori our understanding of the temperature gradients is limited. Figure 3 shows the average values (between low and high instruments) for the wind speed and the temperature on the left graph, and the atmospheric pressure at 2m on the right.

The statistics of the corresponding gradients are shown on Figure 4. For the gradients the Day/Night differences are significantly more pronounced. While there is a marked negative temperature gradient during the day, the night time gradient is lower and positive. The wind gradients show a similar trend but milder. Interestingly, the difference in wind direction between the 10m sensor and the 30m sensor can be significant. For the pressure we only have a sensor at 2m, so the gradient is assumed to be the standard value of $dP/P = -(m_A g/kT)dh$ where for dry air $m_A = 29$amu. Table 1 summarizes the measurements.

In the analysis of the data we should keep in mind that, while the anemometers at 10m and 30m are identical, the device at 20m is a 3D ultrasonic sensor, so there may be systematic calibration differences between the 10m/30m units and the 3D anemometer. In computing the wind speed gradient it is customary to ignore the vertical component, and to consider only the advective terms,

$$dU/dh = \sqrt{[U_x(h_1) - U_x(h_2)]^2 + [U_y(h_1) - U_y(h_2)]^2}$$

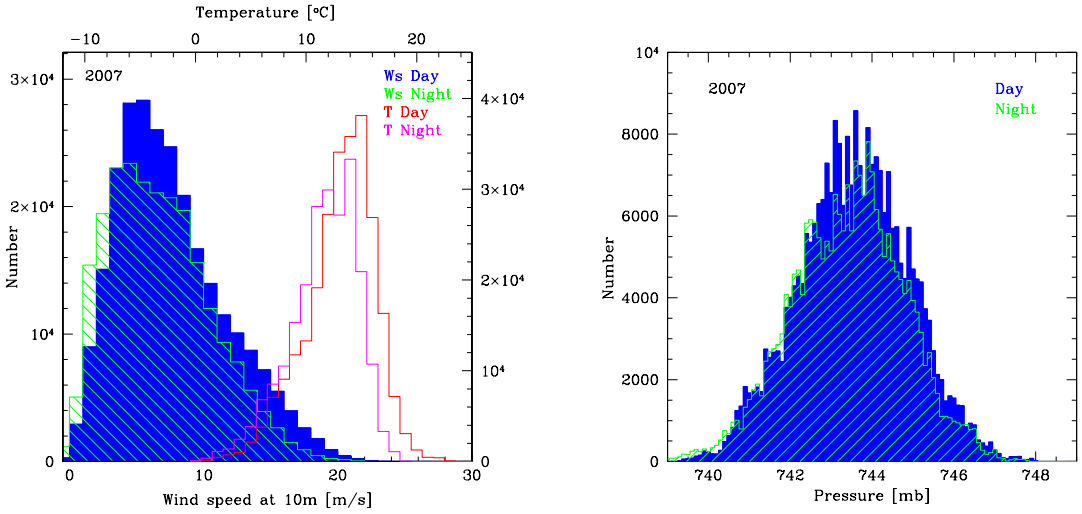

Figure 3: (left) *Statistics of wind speed and temperature on Paranal for the year 2007. The average values at 10m and 30m for the wind, and 2m and 30m for the temperature are shown.* (right) *Statistics of atmospheric pressure 2m above the ground.*

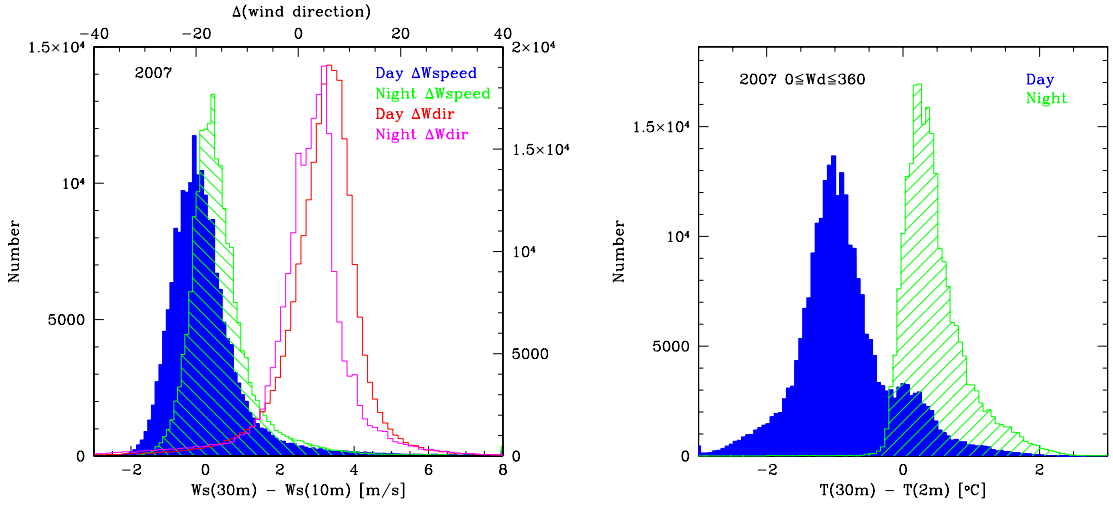

Figure 4: (left) *Statistics of difference in wind speed and wind direction between 30m and 10m over Paranal for the year 2007.* (right) *Statistics of temperature difference between 30m and 2m for 2007. Notice the temperature inversion during night time.*

Table 1: Mean atmospheric parameters over Paranal

Altitude	Temperature [^{o}C] (σ)		Wind Speed [m/s] (σ)		Pressure [mb] (σ)		Relative Humidity [%] (σ)	
	day	night	day	night	day	night	day	night
2m	13.5 (3.2)	11.4 (3.1)	—	—	743.6 (1.3)	743.4 (1.4)	16 (12)	15 (12)
10m	—	—	7.6 (4.1)	6.7 (3.8)	—	—		
20m	—	—	7.7 (3.8)	7.4 (3.8)	—	—		
30m	12.7 (3.0)	11.8 (3.0)	7.7 (4.1)	7.4 (4.1)	—	—	16 (14)	12 (18)

Table 2 shows the resulting gradients in the relevant parameters. Since the anemometers at 10m & 30m are identical, it is safer to use the gradient between them with the caveat that in general the wind speed gradients change with altitude (see below). The yearly average of the night-time Richardson number for the surface layer on Paranal is

Table 2: Average yearly gradients (2007)

Gradient	20m - 10m		30m - 20m		30m - 10(2)m	
	day	night	day	night	day	night
dU/dh (s^{-1})	$+0.10 \pm 0.09$	$+0.10 \pm 0.13$	$+0.08 \pm 0.06$	$+0.10 \pm 0.06$	$+0.07 \pm 0.06$	$+0.06 \pm 0.07$
$d\theta/dh$ (^oK/m)	—	—	—	—	-0.034 ± 0.028	$+0.0174 \pm 0.0174$
dP/dh (mb/m)	-0.090 ± 0.0002					

$$\mathcal{R}_i = \frac{g}{\theta} \frac{\frac{d\theta}{dh}}{(\frac{dU}{dh})^2} = 3.44 \times 10^{-2} \frac{d\theta/dh}{(dU/dh)^2} = 0.19 \pm 0.33(\sigma) \tag{11}$$

just below the "magical" number of $\mathcal{R}_i = 0.25$. Since the dispersion is quite large the conditions of the *surface layer* on Paranal are highly variable: assuming a Gaussian distribution, unstable conditions ($\mathcal{R}_i < 0.25$) occur about 60% of the time while stable conditions ($\mathcal{R}_i > 1$) are very rare. [2] [3] Coincidentally, Figure 6 (see below) indicates that the *inconvenient discrepancy* is statistically small about 10% of the time. This adds plausibility to the argument that a thin, turbulently unstable, but convectively stable surface layer of the atmosphere is responsible for the *inconvenient discrepancy.*

The temperature inversion over Paranal stabilizes the surface layer against convection and is probably responsible for keeping it below 20m height. In fact, a temperature inversion is the standard night time condition over cities and flat-lands and is termed the *Nocturnal Stable Layer (NSL)* by meteorologists. The NSL typically extends a few tens of meters above the ground (Stull, 1988). Figure 5 shows the gradient of temperature (30m-2m) as a function of time in hours from sunset color coded according to the different seasons. The Figure shows that the temperature inversion sets-in shortly after sunset, although conditions may still be unstable up to 2 hours after sunset, specially in winter time. The right panel shows the evolution of the wind-shear between 10m and 30m, which is seen to be remarkably stable throughout the night and the seasons. This remarkable stability is probably what makes Paranal an excellent site for astronomical observation. If only the jet-stream was not overhead, Paranal would be a perfect site in absolute terms. The conditions where the wind speed at 30m is much higher than at 10m will be discussed below.

4.3 The Purple Rose of Paranal

From our previous investigation (Sarazin et al., 2008) we know that the surface layer appears to be particularly active when the wind blows from certain preferential directions. Figure 6 reproduces wind-rose of Paranal coded by the *inconvenient discrepancy, ds* (the difference between the seeing measured by the DIMM and the seeing measured by the UT telescopes to the power 5/3). Shown in light-blue are the wind cones for which $ds > 1''$: NNE ($10^o - 65^o$) and SSE ($140^o - 165^o$).

The wind-rose is somewhat misleading because the density of green/red points in these directions appears to be much larger than it really is, and because the blue points already correspond to a pretty high threshold $ds < 1''$. The right side of Figure 6 shows the distribution of ds for all wind conditions in blue and for NNE winds in green. The cumulative distributions show that the discrepancy is elevated by 10% under NNE conditions. Thus, $ds > 1''$ happens about 20% of the time when the wind blows from the NNE and only 10% of the time for average wind conditions. But these are the extremes; still, more than 60% of the time $ds > 0.5''$ when the wind comes from the NNE!

[2] The stability threshold is experimentally uncertain and the state of the flow in the hysteresis regime (between 0.25 and 1.0) depend on the history.

[3] During day time the temperature gradient is much larger than the adiabatic gradient, so the atmosphere is extremely turbulent. For this reason intrepid French *cooperants* were never allowed to paraglide from La Silla

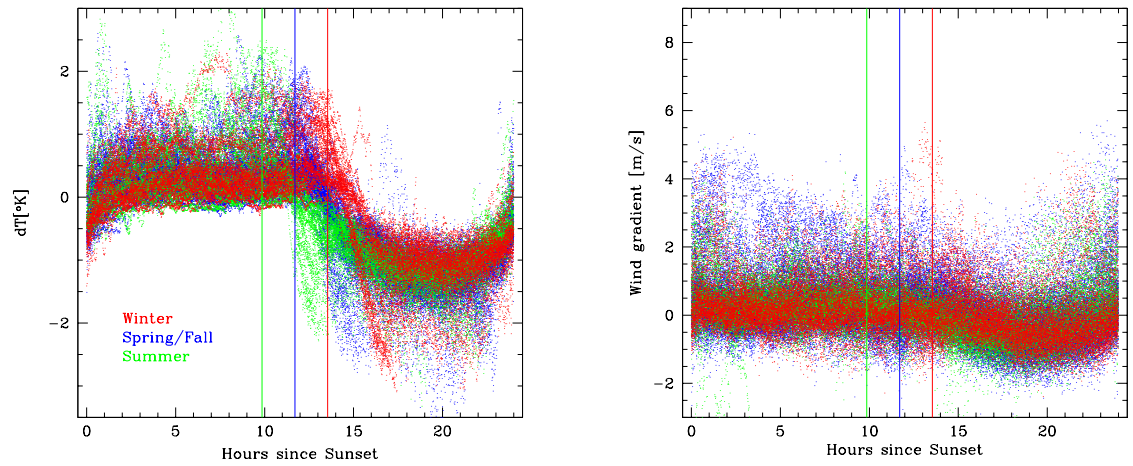

Figure 5: (left) *Temperature gradient (30m-2m) as a function of time since sunset. About one hour after sunset the night time gradient becomes positive (on average). The vertical lines indicate approximate Sunrise times in the four seasons.* (right) *Wind speed gradient between 30m and at 10m as a function of time since sunset. The gradient is seen to be extremely stable during the night showing a very mild trend during daytime.*

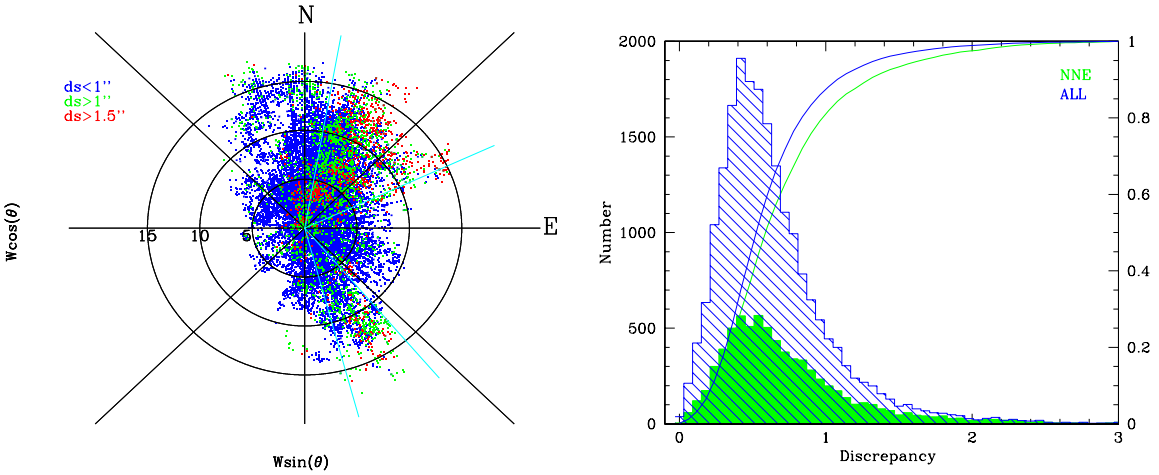

Figure 6: (left) *The Purple Rose of Paranal: The wind-rose coded by inconvenient discrepancy* $ds = (DIMM^{5/3} - UT^{5/3})^{3/5}$. *The light-blue cones delineate the directions for which* $ds > 1''$ *is seen most often: NNE (10-65 degrees) and SSE (140-165 degrees).* (right) *Distribution of ds for the all winds (blue) and for only NNE winds (green). The lines show the cumulative distributions.*

4.4 When East meets West

Figures 7 shows the temperature and wind gradients for NNE conditions. The potential temperature gradient (2m-30m) is $d\theta/dh = 0.022^{o}$K/m and the wind velocity gradient (averaged over the three sensors) is $dU/dh = 0.04 \pm 0.07 s^{-1}$. So for a Gaussian distribution the surface layer is unstable about 70% of the time when the wind blows from the NNE compared to about 60% for average conditions. This happens because although the Richardson number is about two times higher for NNE conditions, the dispersion is much larger (0.6 vs. 0.3). As mentioned above, there is hysteresis in the transition from unstable to stable so it is unclear how to calculate the fraction of the time the surface layer is stable under NNE conditions, but $\mathcal{R}_i > 1$ should occur about 10% of the time which according to Figure 6 correspond to an inconvenient discrepancy of less than 0.2". In other words, $ds < 0.2''$ happens about 10% of the time for NNE winds.

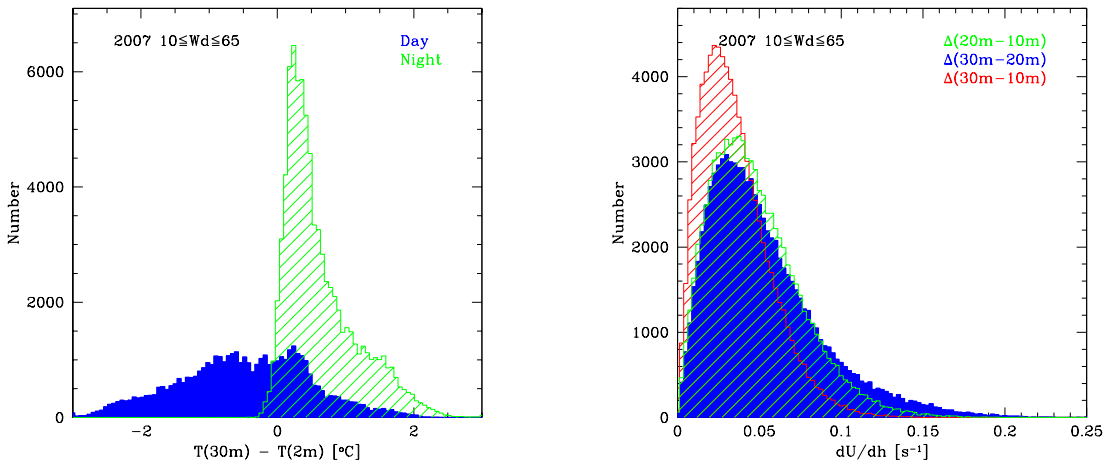

Figure 7: (left) *Statistics of temperature on Paranal for the year 2007 when the wind blows from the NNE (10-65 deg.). Notice that NNE winds are significantly more frequent during the night than during day time.* (right) *Night-time statistics of wind speed when the wind blows from the NNE.*

Figure 8 shows that the situation is radically different for SSE winds. Notice the change in scale! During night time the distribution of temperature gradients is similar to the yearly average (although the mean temperature is $\sim 2^oC$ warmer at night and 2.4^oC during the day; these conditions occur predominantly during the southern summer). The wind speed gradients, however, are much larger. For the 10m-20m layer $d\theta/dh = 0.0234^oK/\mathrm{m}$ and $dU/dh = 0.28s^{-1}$, so for the *surface layer*, $\mathcal{R}_{i,SSE} = 0.01$ (for SSE conditions calibration errors are a small fraction of the gradients). Thus the first 20m above ground are extremely turbulent, as well as the layer between 20m and 30m for which $\mathcal{R}_{i,SSE} = 0.08$. Given that on Paranal the DIMM and the meteorological tower are located in the NNE sector of the observatory, directly in the "von Karman street" of the UT's and VST when the wind blows from the South, it seems clear that the turbulence seen by the DIMM and by the anemometers is due to that wake. This would also explain the fact that the 30m-10m wind gradient distribution is narrower than those involving the 20m wind. There are a number of other statistics that one can do to show that indeed the *inconvenient discrepancy* for SSE winds is local and caused by the perturbation of the UT's on the DIMM. We are left with the problem to explain the inconvenient discrepancy when the wind blows from the NNE.

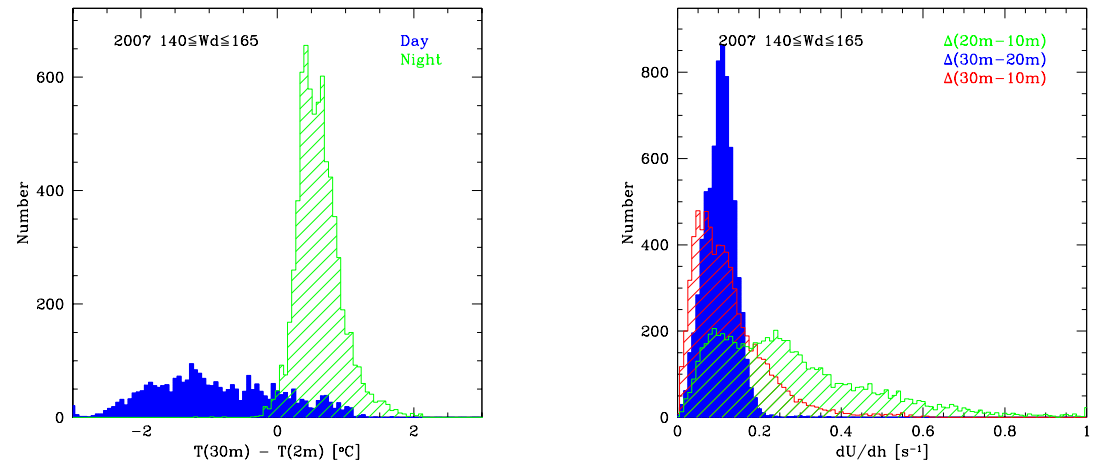

Figure 8: (left) *Statistics of temperature on Paranal for the year 2007 when the wind blows from the SSE (140-165 deg.). Notice that SSE winds are significantly more frequent during the night than during day time.* (right) *Nigh time statistics wind speed when the wind blows from the SSE.*

We should notice that both in NNE and SSE conditions, the potential temperature gradients are larger than the average yearly value with a very small dispersion: whenever the wind blows from these directions there is always a steep temperature gradient! It is interesting therefore to examine what happens when the wind does not blow from these directions. This is explored in Figures 9 and 10 that show the NNW and SSW conditions. Interestingly, for northerly conditions the wind velocity gradients are not much different ($\sim 0.05 s^{-1}$), but the potential temperature gradient is basically zero when the wind blows from the Pacific Ocean (NNW). For southernly conditions, one still sees the effect of the VST and UT4 obstruction, and there is also a sizable temperature gradient, so one would expect *ds* to be enhanced. And again the dispersion in potential temperature gradient is extremely small.

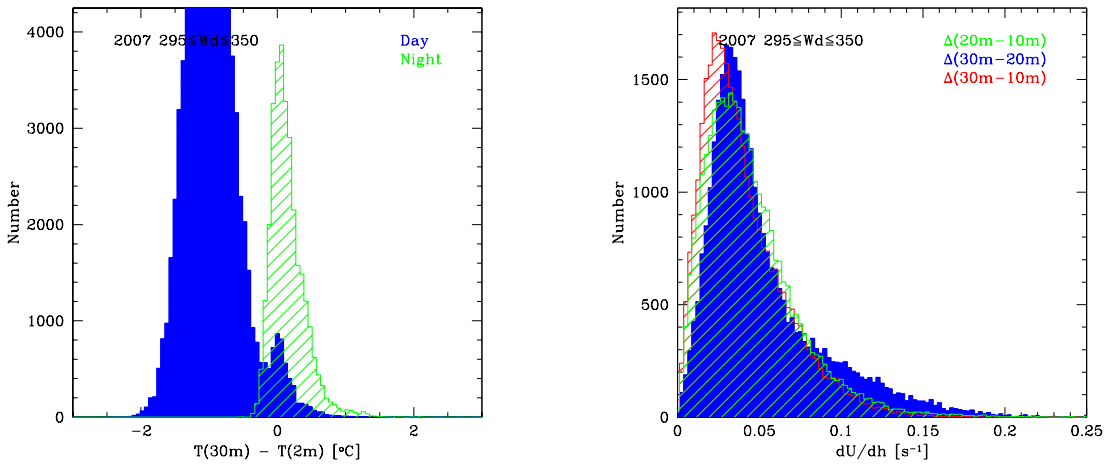

Figure 9: (left) *Statistics of temperature on Paranal for the year 2007 when the wind blows from the NNW (295-350 deg.). Notice that NNW winds are significantly more frequent during the day than during night time.* (right) *Nigh time statistics wind speed when the wind blows from the NNW.*

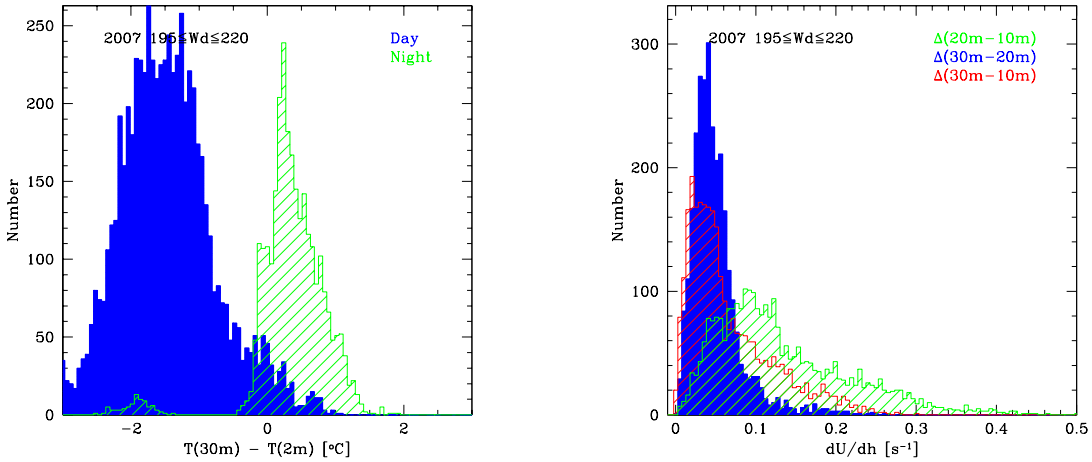

Figure 10: (left) *Statistics of temperature on Paranal for the year 2007 when the wind blows from the SSW (195-220 deg.). Notice that SSW winds are significantly more frequent during the day than during night.* (right) *Nigh time statistics wind speed when the wind blows from the SSW*

Table 4.4 summarizes the relevant parameters of the distributions. The quoted errors correspond to the actual (rms) widths of the distributions to give an indication of the range of conditions encountered throughout the year. In order to interpret these numbers, we should remember that, while Richardson numbers lower than 0.25 signal unstable conditions, when the potential temperature gradient is vanishingly low (such as in the case of

Table 3: When East meets West *

Parameter	NNE ($10^o - 65^o$)	NNW ($295^o - 350^o$)	SSE ($140^o - 165^o$)	SSW ($195^o - 220^o$)
$(dU/dh)_{10m-20m}$	$0.048 \pm 0.028[s^{-1}]$	0.044 ± 0.028	0.280 ± 0.188	0.133 ± 0.083
$(dU/dh)_{20m-30m}$	0.053 ± 0.035	0.052 ± 0.036	0.104 ± 0.038	0.050 ± 0.032
$(dU/dh)_{10m-30m}$	0.035 ± 0.021	0.040 ± 0.026	0.125 ± 0.090	0.067 ± 0.053
$(d\theta/dh)_{Day}$	-0.019 ± 0.038[°K/m]	-0.038 ± 0.016	-0.035 ± 0.037	-0.057 ± 0.027
$(d\theta/dh)_{Night}$	$+0.024 \pm 0.020$	$+0.005 \pm 0.009$	$+0.023 \pm 0.012$	$+0.013 \pm 0.020$
$\mathcal{R}_{i,10m-20m}$	0.36 ± 0.52	0.09 ± 0.20	0.01 ± 0.01	0.02 ± 0.05
$\mathcal{R}_{i,20m-30m}$	0.29 ± 0.48	0.07 ± 0.16	0.07 ± 0.04	0.17 ± 0.29
$\mathcal{R}_{i,10m-30m}$	0.66 ± 0.81	0.11 ± 0.23	0.05 ± 0.04	0.10 ± 0.17

* The $\pm$ values correspond to the 1σ width of the observed distributions.

NNW winds), no matter how turbulent the flow may be, no seeing fluctuations will be observed because there will be no gradients in the index of refraction. Thus, the *inconvenient discrepancy* is low when the wind blows from the NNW due to the stabilizing effect of the ocean. Conversely, the potential temperature gradient is maximal when the wind blows from the "east" (NNE & SSE) which for SSE explains why *ds* is large.

4.5 When South meets North

Figure 11 shows the Paranal wind-rose color coded according to the vertical component of the wind velocity at 20m (U_Z) for 2007 and also for 2000 when the VST dome was not yet there.

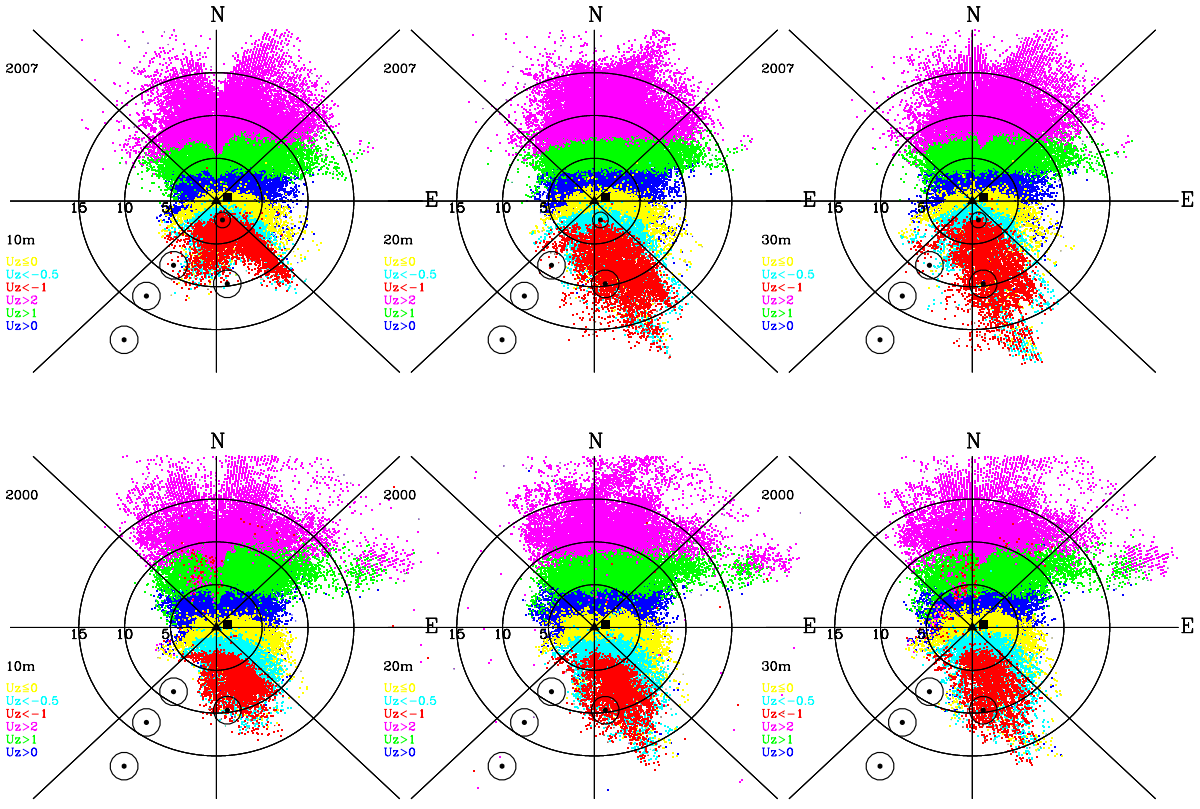

Figure 11: (top) *The wind-rose of Paranal in 2007 color coded according to the vertical component of the wind velocity at 20m (U_Z). The silhouettes show the relevant structures on the Paranal plateau. The weather tower is centered on the plot, and the DIMM is the square just East of the tower.* (bottom) *Same for year 2000 when the VST dome was not there.*

Vertical winds are negative when the wind blows from the south and for weak winds from the north indicating that the flow near the mast is turbulent under these conditions. The substantial similarity between the plots for 2000 and for 2007 indicate that the wind pattern over Paranal has been very stable over the past 8 years, with the clear difference of the disturbances caused by the VST. A close inspection reveals the effect of the UT and VST domes, specially for southernly winds, but possibly also when the wind blows from the North (indicated by an intriguing "dent" in the plots at 10m, which are not visible at 20m and reappear again at 30m, albeit rotated about 10 degrees to the East, both in the 2007 and in the 2000 plots). These plots clearly explain the enhanced inconvenient discrepancy for SSE winds, but what about NNE? The vertical component at 20m is always rising for winds blowing from the NNE except when the wind is weak ($< 1m/s$) where it appears to be falling. The Paranal top drops sharply at the position of the weather tower, and it is natural to expect winds to be rising when they blow from the NNE-NE. Can this rising component be related to the inconvenient discrepancy?

4.6 Seeing is Believing

We can use the *inconvenient discrepancy (ds)* itself to quantify the influence of winds on the surface layer. When UT data are not available we can rely on the comparison between MASS and DIMM to estimate *ds*. Figure 12 compares two very different nights. The left shows a good night: the temperature at 2m dropped sharply about 2hrs after sunset causing the DIMM and MASS seeing to rise up to 3". During the first two hours the wind was blowing from the SSE and was very turbulent at all heights. Then the wind turned sharply to the South, the temperature gradient dropped, the winds died down and the seeing was very good with a small difference between UT2 and the DIMM. The right hand plot shows the opposite situation: during the first couple of hours the wind is blowing from the North to the East and there is a mild temperature gradient. The seeing is not too good, but the discrepancy is weak. Two hours after sunset the wind turns to the NNE, the temperature at 2m drops compared to the 30m temperature, and both the DIMM and the MASS seeing simultaneously rise to about $2''$. The seeing at UT2, however, stays the same. Both the 2m and 30m temperatures continue to drop and about 5hrs from sunset the wind turns about 20 degrees to the North, the 2m temperature drops faster than the 30m temperature, and the DIMM seeing jumps to more than $3''$ while the MASS and UT2 remain where they were. The wind speed increases above 10m/s and is very turbulent, and when it starts blowing from about 10 degrees (NNNE), the temperature gradient drops and while the wind remains strong and turbulent, the DIMM seeing drops to the level of the MASS and UT1, but only for a brief time. The wind eventually turns east and again a temperature gradient develops that causes the DIMM and the MASS to raise well above UT2. Throughout this night, the surface layer is clearly running the show, so it is quite surprising to see that at times the MASS follows the DIMM rather than following UT2 or doing something else.

The comparison of these two plots illustrate the following general features: (We have selected several plots representative of these regularities. These are presented in the Appendix and the brave reader is gently encouraged to scan these plots to recognize these and surely other regularities that we may have missed.)

- The temperature gradient increases when the wind blows from the NNE-NE directions. This increase is due to a drop in the temperature at 2m, and not to an increase of the temperature at 30m.
- The wind at 10m is generally significantly slower and more turbulent than at 20m and 30m when the wind blows from the South. While the temperature gradients for southernly winds tend to be smaller and the wind speed gradients larger, there is no clear trend between these variables and the inconvenient discrepancy. Strong southernly winds are extremely turbulent as the UT's and the VST stand directly upwind from the weather mast.
- The 10m wind speed is clearly slower when the wind blows from due North, which could be an effect of the buildings since the drop appeared in 1998 and was not present before (see below). Even in the presence of significant wind shear and turbulence, the seeing can still be good if the temperature gradient is small. But when the wind blows from the NNE, the inconvenient discrepancy can be very large even with low temperature gradients.
- The wind speed plays a clear role in stirring the surface layer. Winds stronger than about 10m/s are very turbulent and even a small temperature gradient is enough to elevate the inconvenient discrepancy. Occasionally the temperature inversion disappears during night-time and the surface layer becomes instantly convective.

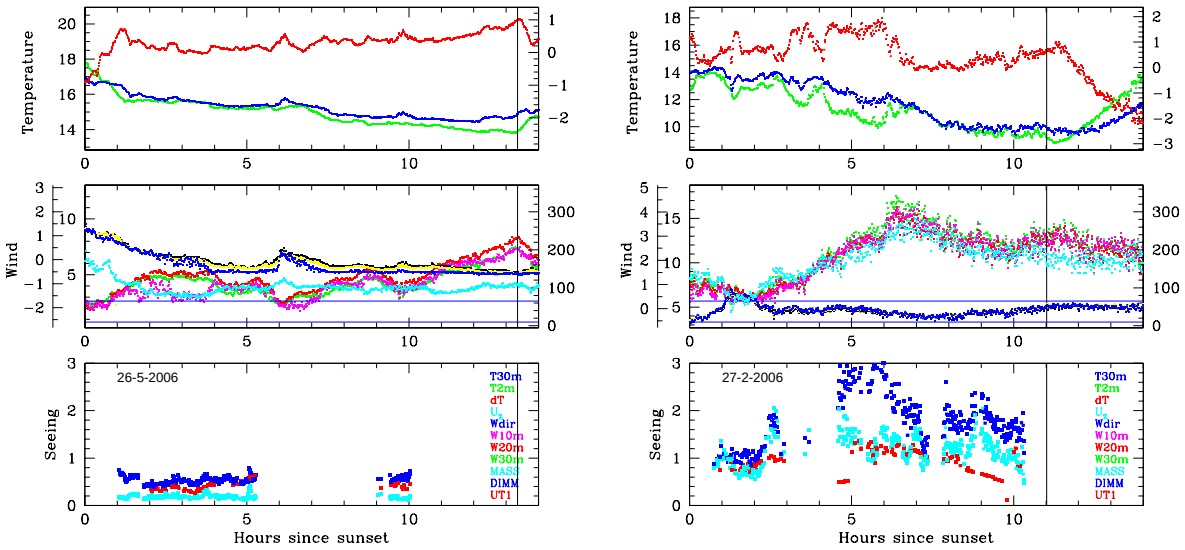

Figure 12: *Synoptic weather plot for a given night on Paranal. The top panel shows the temperature at 2m (T2m; green), and 30m (T30m; blue) and the difference dT=T30m-T2m in red. The middle panel shows the wind speed at 10m (magenta), 20m (red), 30m (green) and the vertical wind speed at 20m (cyan). The inner scale on the left of the panel shows the horizontal speeds and the outer scale the vertical speed. The wind direction at the three altitudes is shown as black, yellow, and blue and the scale is on the right of the panel. Most of the time the three directions coincide so only the blue curve (20m) is visible. The thin lines indicate the wind directions of maximum inconvenient discrepancy (NNE-NE: 10-65 degrees). The lower panel shows the seeing measured by the DIMM (blue), the MASS (cyan) and the Shack-Hartmann sensor on UT2 (red). The vertical line on each panel indicates the sunrise.* **(left)** *A good night: after a very turbulent beginning (0-2 hours after sunset) the wind suddenly turned to the South and the temperature gradient dropped significantly below* 1^oC*; the seeing improved dramatically.* (right) *A bad night: the wind was blowing from the NNE and the temperature gradient was quite high and there was also a significant wind gradient. Notice that about 7 hours after sunset the temperature gradient dropped momentarily to almost zero and so did the inconvenient discrepancy.*

4.7 When Cold meets Warm

We conclude from the preceding discussion that the *inconvenient discrepancy* arises when cold air from the valleys is advected to the Paranal summit by NNE-NE winds. This generates a thermal gradient over the first 30m which is mixed by wind shear and turbulence to generate optical turbulence. Let us examine the evidence for that conclusion. Figure 13 shows on the left panel the Purple-Rose of Paranal color coded by the temperature gradient between 30m and 2m. The greatest temperature gradient is advected to Paranal by NE winds, but the cone of high ΔT spans more than 50 degrees about the NE direction. The right panel shows the purple-rose color coded by the variance of the wind speed measured at 20m.[4] We see that the wind is most turbulent when it blows from the NNE (and from the S-SSE where the effect of the VST dome is clearly seen). These figures clearly show that the combination of temperature gradient and high wind turbulence are the cause of the *inconvenient discrepancy*.

We have seen that the temperature gradient is due to cold air from the valleys advected by the wind to Paranal. But, why are the temperature and turbulence vectors misaligned? The MIM simulations computed by meteorologists in the University of Munich under contract with ESO may offer at least part of the answer. Figure 14 show the reconstruction of the wind direction for three simulations for September 1999. The simulations show that winds generally travel a rather long distance over ground before arriving on Paranal, and that the direction of arrival is not always the long-range direction of departure. Over ranges of 40-60km, however, the winds arrive straight on Paranal, so we suggest that the source of turbulence lies in the orographic conditions upwind from the summit. And there are plenty including La Montura and VISTA peak, among others.

[4]The wind-speed sensors are read every 2s and the variances are logged together with the mean speeds every 60s. The sonic sensor at 20m has a higher bandwidth than the standard (spin wheel) anemometers at 10m and 20m, and therefore we have retained the variance at 20m, but the other sensors show essentially the same features.

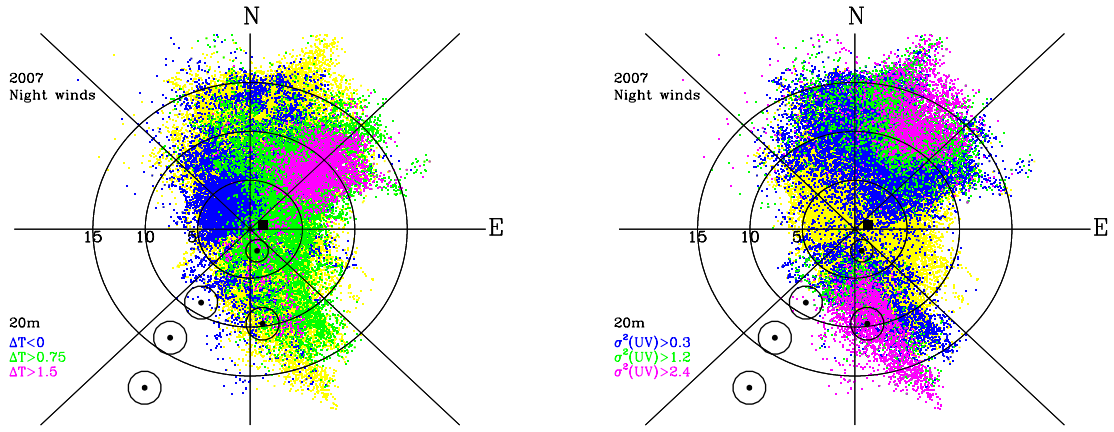

Figure 13: (left) *The 2007 wind-rose of Paranal at 20m color coded according to the temperature gradient between 2m and 30m,* $\Delta T = T30m - T2m$. *Yellow indicates* $0 < \Delta T < 0.75$. (right) *Color coded according to the variance of the horizontal wind velocity at 20m* (σ^2). *The silhouettes show the relevant structures on the Paranal plateau. The weather tower is centered on the plot, and the DIMM is the square just East of the tower. Notice the misalignment between the maximum temperature gradient and the maximum wind turbulence.*

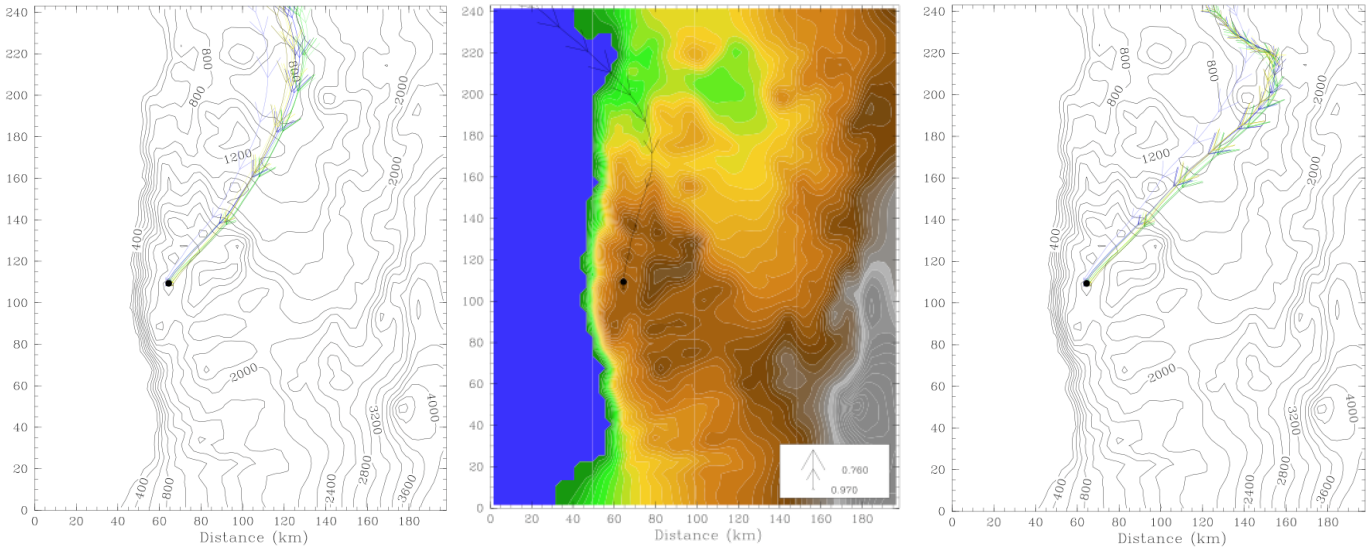

Figure 14: *These simulations from the University of Munich show that the wind travels a long distance over land before arriving on the Paranal summit, and that the direction of arrival is generally different from the direction the wind came from in the long range.*

4.8 The Power of the Surface Layer

Comparing DIMM with MASS one can get a pretty good idea of the ratio of turbulent energy between the ground layer and the free atmosphere as,

$$\frac{C_n^2(BL)}{C_n^2(Tot)} = 1 - \frac{\epsilon_{MASS}^{5/3}}{\epsilon_{DIMM}^{5/3}}$$

The distribution is shown in Figure 15. The median value is 64% and we know from the SLODAR measurements

(Sarazin et al., 2008) that about 78% of the energy is in the first SLODAR layer $h < 94m$, so we get an upper limit of about 50% for the turbulent energy of the surface layer. We can get even closer if we use the UT seeing instead of the MASS. Comparing UT with DIMM we get the fraction of the turbulent energy that is *not* seen by the UT's. This is shown by the green curve in Figure 15. The median value is 48% indicating that indeed most of the boundary layer energy is in the surface layer.

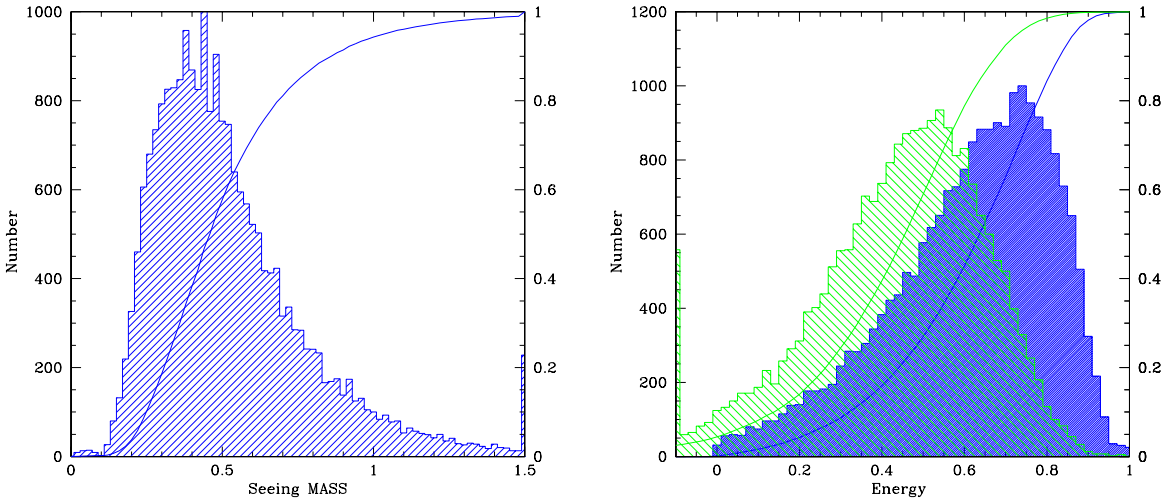

Figure 15: (left) *Seeing distribution measured by MASS (free atmosphere)* (right) *Fraction of the total turbulent energy of the atmosphere that comes from the boundary layer (Blue) and from the surface layer (Green).*

4.9 Kolmogorov meets von Karman

The gentle reader is referred to the paper by Tokovinin (2002) for a summary of the von Karman model and his (Tokovinin's) approximation to compute the seeing measured by (reasonably) large telescopes in the von Karman model. The von Karman model introduces an additional parameter: the wave-front outer scale L_0, and Tokovinin claims that for $L_0/r_o > 20$ the expression

$$\frac{\epsilon_{\rm vK}}{\epsilon_{\rm Ko}} = \sqrt{1 - 2.183 \left(\frac{r_o}{L_0}\right)^{0.356}} \tag{12}$$

is an excellent approximation for the ratio of seeing in the von Karman model to the seeing in the Kolmogorov model. This formula predicts a dependence of seeing with wavelength, which is much steeper than the $\epsilon_{Ko} \propto \lambda^{0.2}$ for pure Kolmogorov turbulence (ie. $L_0 = \infty$). Tokovinin, Sarazin, and Smette (2007) analyzed images obtained with VISIR at 8.6μ and concluded that the von Karman model fits the data reasonably well, albeit with very uncertain values for L_0 which ranged from 20m to about 100m between different exposures separated by fractions of an hour. These fluctuations are not surprising if one considers that most of the time VISIR is diffraction limited already at 8.6μ, while their large fluctuations were observed at longer wavelengths where their method based on ratios in Fourier space is extremely sensitive to noise. However, the very fact that an 8.2m telescope is diffraction limited at 8.6μ provides strong evidence for a finite outer scale!

Figure 16 shows a plot of the mean seeing measured by FORS1, FORS2, ISAAC and VISIR during regular operations. The values have been obtained as follows: QC1 data from the ESO archive were downloaded and filtered to ensure uniform quality in terms of exposure times, air-masses, rejection of non-stellar objects, etc. The FORS1 and FORS2 data covered a period of 8 years (April 2000 to April 2008); ISAAC almost 6 years (July 2002 to April 2008); and VISIR 2.5 years (August 2005 to April 2008). The time series were binned every hour and the bins were averaged over the full period. The mean errors shown in the figure are the standard deviations divided by the square root of the number of measurements, which is of course very large. For each instrument and wavelength (UBVRIz for FORS1; BVRIz for FORS2; JHKs for ISAAC; and 8.6μ PAH for

VISIR) the figure shows three sets of points corresponding to the raw averages (top points); the raw averages corrected for telescope diffraction $\epsilon_{\rm diff} = 1.22\lambda/D$ (middle point); and corrected for diffraction and instrumental resolution assuming 1 pixel FWHM (lower points). The latter correction was not applied to the VISIR point which is already near zero. The green symbols correspond to FORS1 and the black ones to FORS2 at the relevant wavelengths.

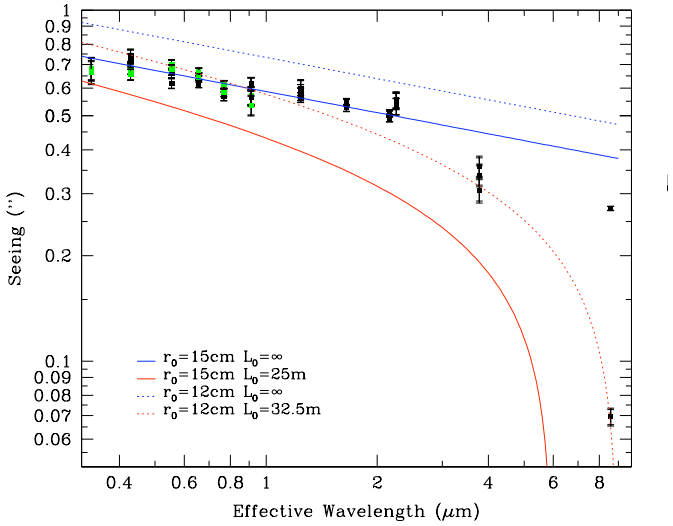

Figure 16: *Seeing as a function of wavelength on Paranal. The UBVRI data are from 8 years of archival (QC) FORS1 (green) and FORS2 (black) observations. The JHK$_S$L data are from 6 years of ISAAC QC data; and the 8.6μm are from 2.7 years of VISIR archival data. For each instrument there are three sets of points corresponding to the raw averages (top); seeing corrected for diffraction limit (mid); and seeing corrected for diffraction and intrinsic image qualities (bottom). The last correction was not applied to the VISIR data that are mostly diffraction limited. The curves for $L_0 = \infty$ correspond to the Kolmogorov cascade ($\epsilon_{\rm Ko} \propto \lambda^{-0.2}$). The curves for finite L_0 correspond to the Von Karman model.*

The 4 curves shown in the figure are not fits; the parameters were simply chosen to illustrate plausible values. The ISAAC L and VISIR 8.6μ points provide strong constraints, but unfortunately are rather uncertain: the JHKs points are significantly above the red dotted curve indicating that there may be a problem with the ISAAC optics. In the case of VISIR, even a minute correction for instrumental resolution will move the point to imaginary values. But clearly the average value of L_0 cannot be very different from 30m. Even $L_0 = 25$m is seen to be a poor match to the data. Interestingly, the von Karman/Tokovinin model does not seem to fit the blue (U,B) and the red (L,8.6μ) extremes of the data at the same time. The presumed internal image quality problems of ISAAC prevent us from a finer analysis, which should be resumed when HAWK-I data become available. Still, the L-band point is crucial, so it is very important to understand whether the ISAAC point can be trusted.

5 Epilogue: Gone with the Wind

The Purple Rose of Paranal changed suddenly in 1998. From the beginning of the site-testing campaign until 1997, the wind-rose remained essentially identical to the one shown in Figure 17 for 1997, but in 1998 it suddenly changed and, as discussed above, has remained essentially unchanged ever since.

The NNW winds that predominated before 1998 are less turbulent and, as we saw before, do not advect cold air from the valleys, so the DIMM was not affected by local (optically) turbulent conditions. In 1998 conditions changed and the predominant winds started to blow from the NNE, which not only are significantly more turbulent than the NNW winds, but also advect cold air from the valleys. As a result, a thin layer of optically turbulent atmosphere sets-in on Paranal, which significantly degrades the DIMM seeing, but is not seen by the VLT Unit Telescopes giving rise to the *inconvenient discrepancy*. We are thus left with two tantalizing questions:

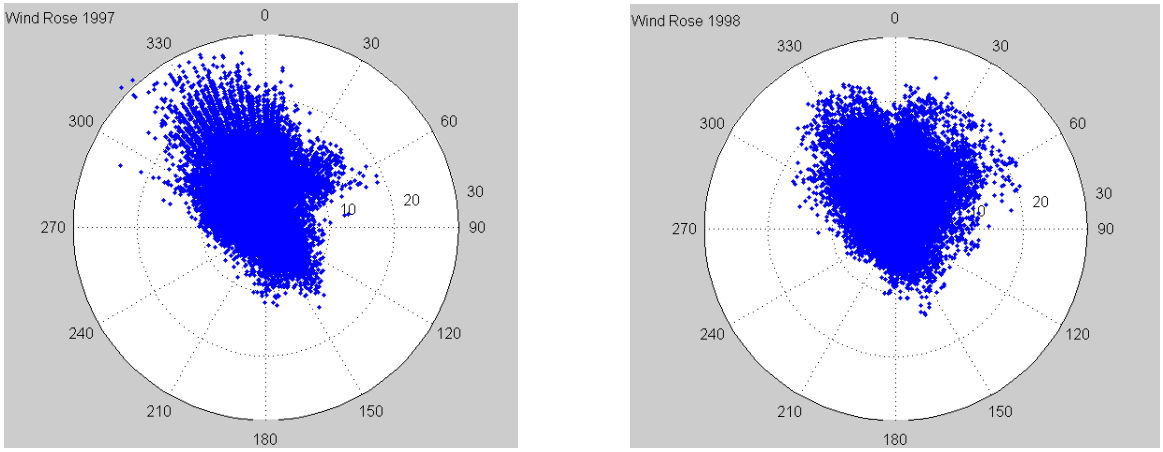

Figure 17: (left) *Wind-rose of Paranal in 1997* (right) *Wind-rose of Paranal in 1998.*

1. What caused the 1998 change of the Purple Rose of Paranal? And,
2. Does the thin layer of optically turbulent atmosphere extend over the whole summit, or does it affect only the immediate surroundings of the DIMM (and the weather mast)?

In a way the two questions are related: the wind-rose of Paranal's "twin" site Armazones does not seem to have changed (at least not significantly) since 1990. This suggests that the 1998 flop of Paranal may not have been due to the enormous El Niño of 1997/1998, which apparently did not affect Armazones. Also, there have been several El Niño-La Niña cycles since 1998, which however do not seem to have affected the Paranal (or Armazones) winds in any significant way. The other important change that occurred in 1998 is that the last large structure on the Paranal summit (UT4) was completed, suggesting that perhaps the extensive "landscaping" of the mountain played a role in affecting the wind patterns. If this is the case, it may be that indeed the *inconvenient discrepancy* is local to the DIMM, and is not present elsewhere on the platform. It should be relatively easy to test this hypothesis using the portable DIMM (the same one that was used on the roof of the VST dome). This experiment is planned for October/November 2008.

It is important to notice that the wind-roses of Paranal and Armazones were significantly different already in 1990: while Paranal had predominant NNW winds, on Armazones the predominant winds came from the NNE. This is relevant because the Armazones and Ventarrones appear to have very similar wind patterns.

6 Acknowledgments

JM thanks Jean Vernin for sharing his wisdom and lecture notes on the very subject of this investigation.

7 Bibliography

1. Schwarzchild, M., (1958) *Structure and Evolution of the Stars,* Dover.
2. Tatarski, V.I., (1961) *Wind Propagation in a Turbulent Medium,* McGraw-Hill.
3. Stull, R.B. (1988). *An Introduction to Boundary Layer Meteorology;* Kluwer.
4. Coulman, C., Vernin, J., & Fuchs, A., (1995), *Appl. Optics,* 34, p.3461.
5. Sarazin, M., Melnick, J., Navarrete, J., Lombardi, G (2008) *The Messenger* 132, p11
6. Riemer, M., & Zängl, G., (2002), *Analysis of the performance of the MM5 for the VLT site at Paranal.*

8 Appendix

8.1 Seeing plots for Paranal

Snapshots of the temperature, wind, and seeing variations during selected nights in 2006. These graphs are representative of the conditions encountered throughout the year, and illustrate the regularities described in the text.

- The temperature gradient increases when the wind blows from the NNE-NE directions. This increase is invariably due to a drop of the temperature at 2m.

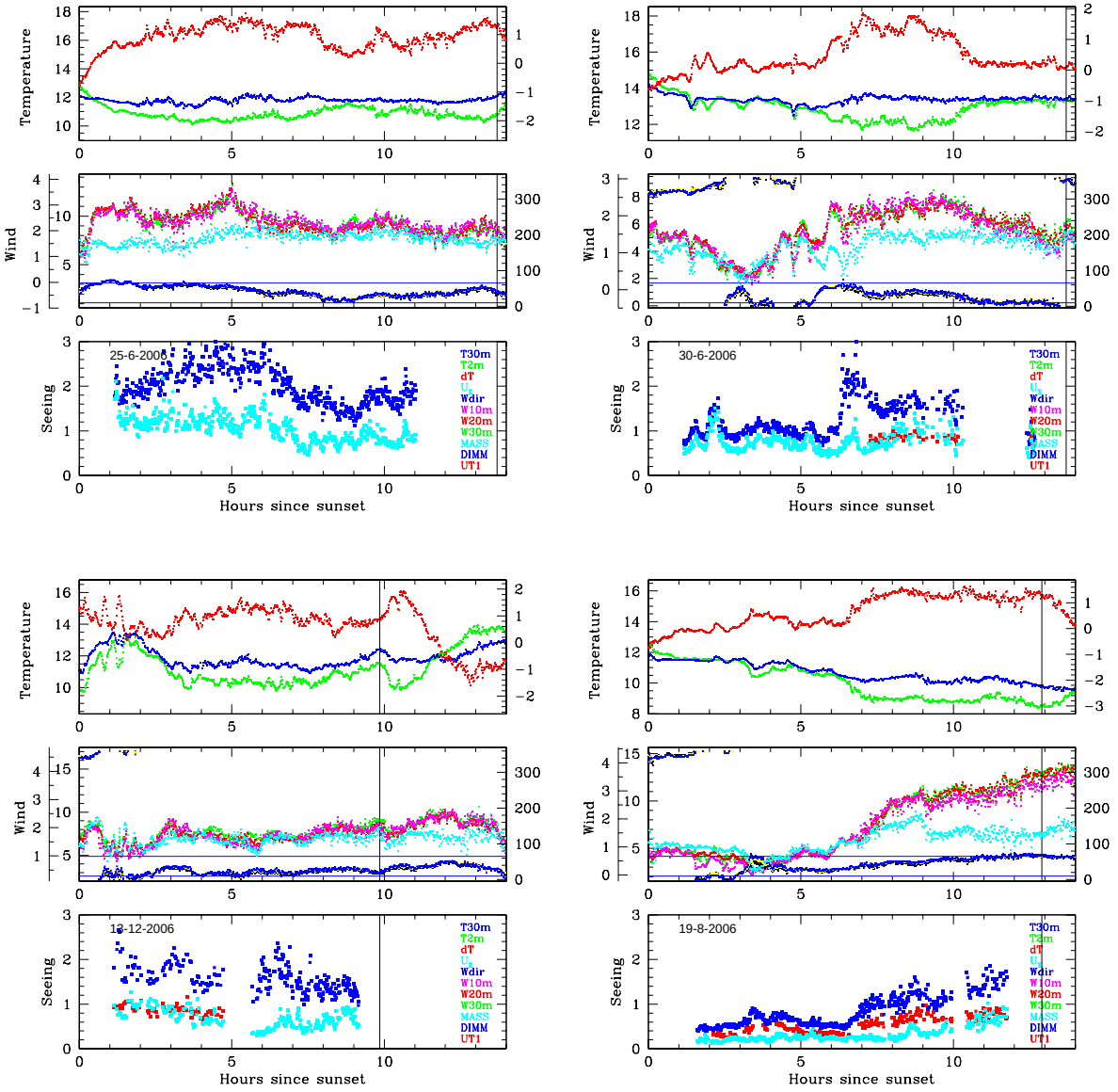

Figure 18: *Same as Figure 12 illustrating the change of temperature at 2m when the wind comes from the NNE-NE direction. The 4 examples show different configurations. The correlations between temperature gradient, wind shear, and seeing are very clear in this plot: when the temperature gradient is strong, even weak winds will generate significant discrepancies, and vice-versa.*

- The wind at 10m is generally significantly slower and more turbulent than at 20m and 30m when the wind blows from the South. While the temperature gradients for southernly winds tend to be smaller and the wind speed gradients larger, there is no clear trend between these variables and the inconvenient discrepancy. Strong southernly winds are extremely turbulent as the UT's and the VST stand directly upwind from the weather mast.

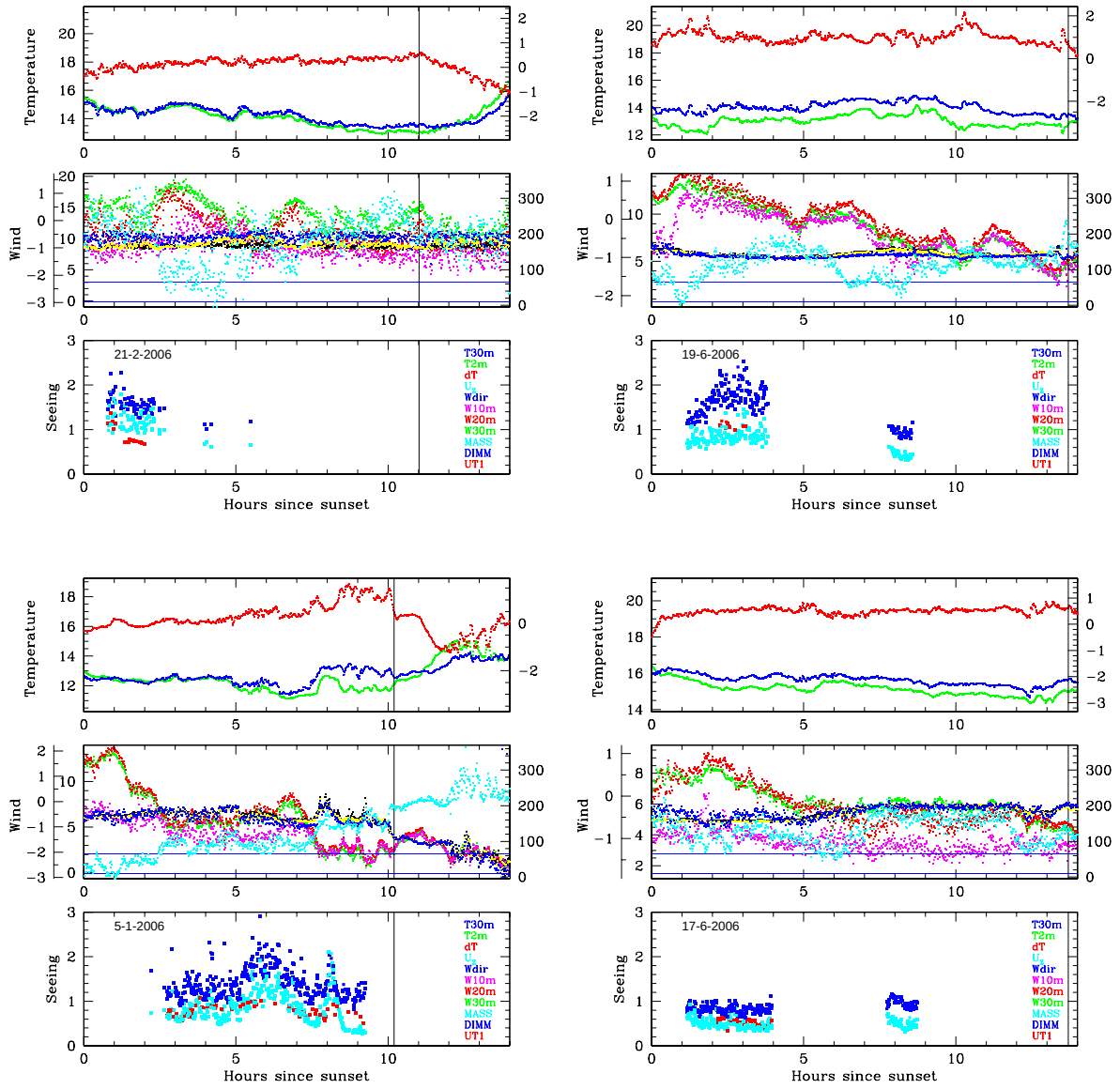

Figure 19: *Same is Figure 12 illustrating the properties of southernly winds. The effects of the wakes of the UT's and particularly VST are clearly seen in this Figure. Strong southernly winds are extremely turbulent, but the temperature inversions tend to be weak. This figure provides further examples of the correlation between wind, temperature, and seeing.*

- The 10m wind speed is clearly slower when the wind blows from the North. Even in the presence of significant wind shear and turbulence, the seeing can still be good if the temperature gradient is small. But when the wind blows from the NNE, the inconvenient discrepancy can be very large even with very low temperature gradients.

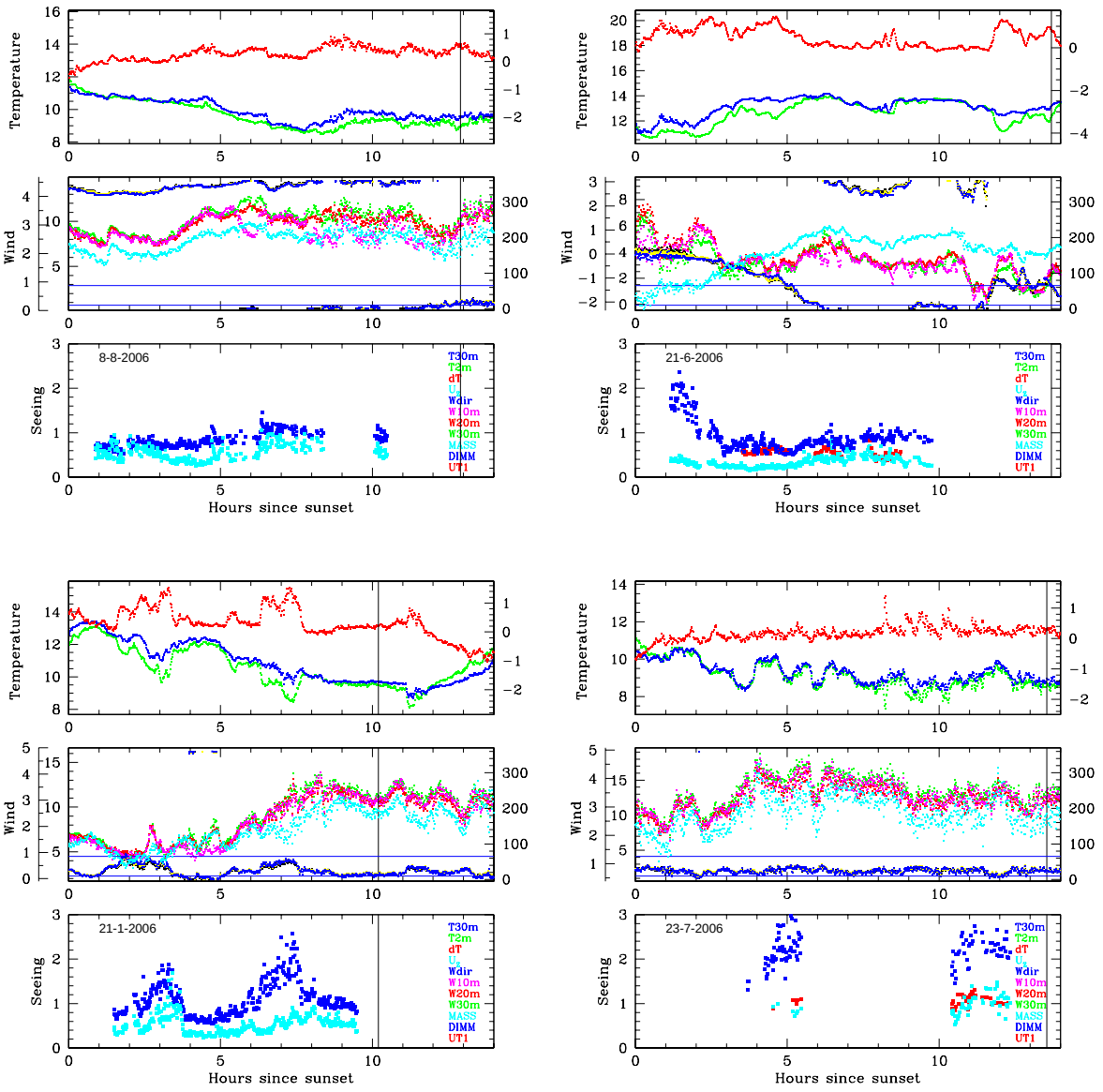

Figure 20: *Same as Figure 12 for Northernly winds. The behavior of the anemometer at 10m could be due to the influence of the VST dome. The seeing is generally good for N wind conditions and the inconvenient discrepancy nominal (*$< 0.5''$*). The large discrepancy shown in the lower-right figure is difficult to explain because the temperature gradient is very close to zero, but notice however that the wind speed is very high and the winds are extremely turbulent. In these cases knowledge of the temperature at intermediate heights (10m & 20m) is essential.*

- The wind speed plays a clear role in stirring the surface layer. Winds stronger than about 10m/s are very turbulent and even a small temperature gradient is enough to enhance the inconvenient discrepancy. Occasionally the temperature inversion disappears during night-time and the surface layer becomes instantly turbulent.

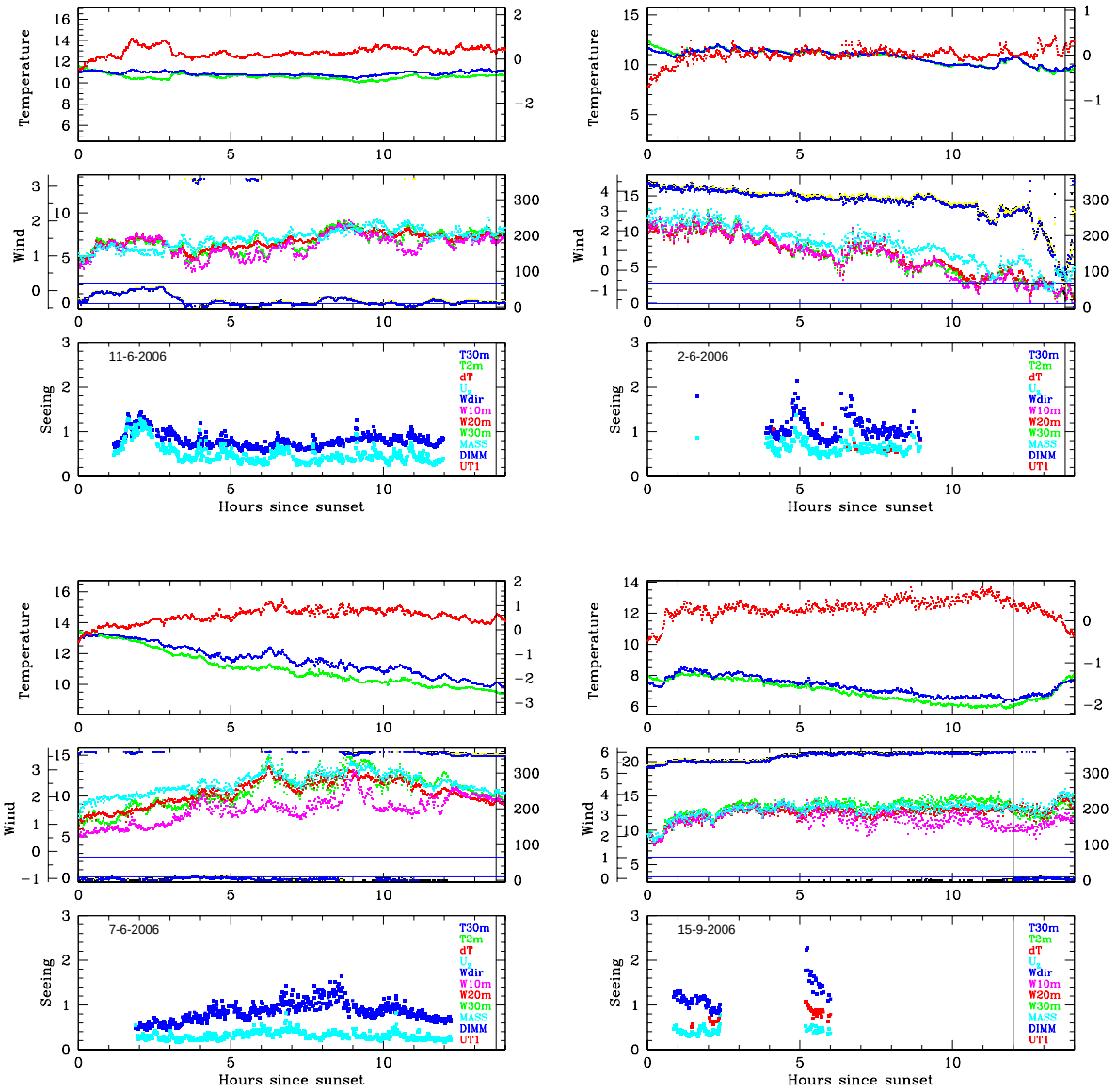

Figure 21: *Same as Figure 12 for an assortment of different conditions. The temperature inversion can disappear giving rise to convection. Strong winds are turbulent and elevate the inconvenient discrepancy in the presence of weak temperature gradients.*